AD-A044 395 NAVAL POSTGRADUATE SCHOOL MONTEREY CALIF F/G 20/4
A THEORY FOR CAVITATION IN IMPELLERS.(U)
JUL 77 C J GARRISON
UNCLASSIFIED NPS-69GM77082 NL

| OF |
AD
A044395

END
DATE
FILMED
10-77
DDC

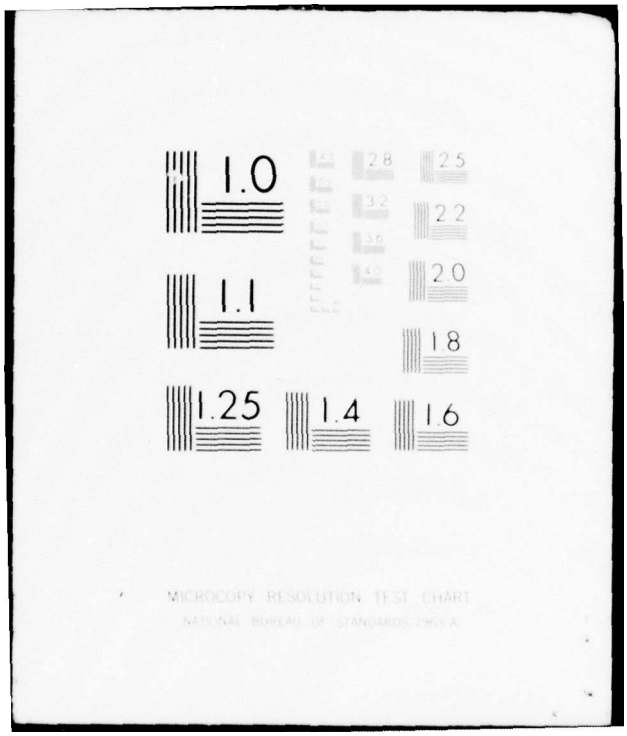
1.0
1.1
1.25
1.4
1.6
2.8
2.5
3.2
2.2
3.6
2.0
4.0
1.8
MICROCOPY RESOLUTION TEST CHART
NATIONAL BUREAU OF STANDARDS 1963 A

NPS69Gm77082

NAVAL POSTGRADUATE SCHOOL

Monterey, California

A THEORY FOR CAVITATION IN IMPELLERS

By

C. J. Garrison

July 1977

NAVAL POSTGRADUATE SCHOOL
Monterey, California

Rear Admiral Isham Linder
Superintendent

J. R. Borsting
Provost

The work reported herein was supported by various Department of Defense activities and the National Science Foundation.

This report was prepared by:

C. J. Garrison
C. J. Garrison
Associate Professor of
Mechanical Engineering

Reviewed by:

Allen E. Fuhs
Allen E. Fuhs, Chairman
Distinguished Professor of
Mechanical Engineering

Allen E. Fuhs for
Robert R. Fossum
Dean of Research

SECURITY CLASSIFICATION OF THIS PAGE (When Data Entered)

REPORT DOCUMENTATION PAGE

READ INSTRUCTIONS BEFORE COMPLETING FORM

1. REPORT NUMBER: NPS69Gm77082	2. GOVT ACCESSION NO.
3. RECIPIENT'S CATALOG NUMBER	
4. TITLE (and Subtitle): A THEORY FOR CAVITATION IN IMPELLERS.	5. TYPE OF REPORT & PERIOD COVERED: Final report.
6. PERFORMING ORG. REPORT NUMBER	
7. AUTHOR(s): C.J. Garrison	8. CONTRACT OR GRANT NUMBER(s)
9. PERFORMING ORGANIZATION NAME AND ADDRESS: Naval Postgraduate School, Monterey, California 93940	10. PROGRAM ELEMENT, PROJECT, TASK AREA & WORK UNIT NUMBERS
11. CONTROLLING OFFICE NAME AND ADDRESS	12. REPORT DATE: July 1977
	13. NUMBER OF PAGES: 36
14. MONITORING AGENCY NAME & ADDRESS (if different from Controlling Office)	15. SECURITY CLASS. (of this report): Unclassified
	15a. DECLASSIFICATION/DOWNGRADING SCHEDULE

16. DISTRIBUTION STATEMENT (of this Report)

DISTRIBUTION STATEMENT A
Approved for public release;
Distribution Unlimited

17. DISTRIBUTION STATEMENT (of the abstract entered in Block 20, if different from Report)

18. SUPPLEMENTARY NOTES

19. KEY WORDS (Continue on reverse side if necessary and identify by block number)

Cavitation
Pump impellers
Potential flow

20. ABSTRACT (Continue on reverse side if necessary and identify by block number)

An approximate theory for cavitation in pump impellers is developed on the basis of a one-dimensional potential flow model. The theory incorporates the unsteady term occurring in Bernoulli's equation and accounts for blockage effects due to vane thickness. A comparison of the theoretical results with experimental data from mixed flow impeller tests shows good agreement near the condition of zero incidence. On the basis of the theoretical results a mechanism of cavitation breakdown is proposed.

DD FORM 1 JAN 73 1473 EDITION OF 1 NOV 65 IS OBSOLETE
S/N 0102-014-6601 |

SECURITY CLASSIFICATION OF THIS PAGE (When Data Entered)

ACKNOWLEDGEMENTS

This investigation was inspired by a course in cavitation taught at the University of Washington in the Department of Civil Engineering by Professor R. E. Nece in 1968.

ABSTRACT

An approximate theory for cavitation in pump impellers is developed on the basis of a one-dimensional potential flow model. The theory incorporates the unsteady term occurring in Bernoulli's equation and accounts for blockage effects due to vane thickness. A comparison of the theoretical results with experimental data from mixed flow impeller tests shows good agreement near the condition of zero incidence. On the basis of the theoretical results a mechanism of cavitation breakdown is proposed.

NOMENCLATURE

A_o = pipe area upstream of impeller, ft.^{2}

A_1 = area of flow passage at the impeller eye without vanes, ft.^{2}

B_v = vane blockage coefficient, dimensionless

$C_v = \frac{1}{1-B_v}$ = vane coefficient, dimensionless

C_s = shroud coefficient, dimensionless

C_m = meridional velocity, ft/sec.

D = impeller diameter, ft.

g = gravitational constant, ft/sec.^{2}

H_{sv} = net positive suction head, ft.

K = cavitation index, dimensionless

N = impeller rotative speed, rpm

P = pressure, lb/ft.^{2}

P_v = vapor pressure, lb/ft.^{2}

$\bar{q}$ = velocity vector, ft/sec.

Q = flow rate, ft^3/sec.

t = time, seconds

u = impeller wheel speed, ft/sec.

Z = number of impeller vanes

α = relative flow angle, radians

β = vane angle, radians

$\bar{\zeta}$ = vorticity vector, sec.$^{-1}$

τ = blade thickness, in.

$\phi = C_m/u$, flow coefficient, dimensionless

Φ = velocity potential, ft^2/sec.

SUBSCRIPTS

0 = reference station upstream of the impeller

1 = reference station outside vane row at impeller inlet

2 = reference station inside vane row at impeller inlet

A THEORY FOR CAVITATION IN IMPELLERS

INTRODUCTION

It has long been recognized that the flow in turbomachinery is by nature unsteady when viewed from a fixed reference frame. Dean [1] pointed out the necessity of unsteadiness by showing that Bernoulli's equation, applied between the inlet and outlet of a pump, denies the addition of energy to the fluid unless the unsteady terms are included. In other words, energy cannot be added to a steady, irrotational flow of a frictionless fluid; only by making the boundary conditions unsteady is it possible to add energy to the fluid.

As a consequence of the inherent unsteady flow occurring in impellers when viewed from a fixed reference frame, it is necessary to account for the unsteady effects in any theoretical attempt to predict cavitation or minimum pressure coefficient. Accordingly, the object of this paper is to develop a theory for cavitation in pump impellers which accounts for such effects. Bernoulli's equation is applied to the flow in the inlet region of an impeller and the unsteady term occurring therein is retained. An analysis is then developed to approximate this term so that the final result yields the cavitation index as a function of the flow coefficient.

One of the most surprising results of this analysis is that the unsteady term in Bernoulli's equation is not of secondary importance but has a major influence on the pressure in the inlet region at values of the flow coefficient on either side of the zero incidence condition. Moreover, on the basis of the

theoretical results obtained, a mechanism for cavitation breakdown at positive and negative incidence conditions is proposed.

The underpressure in the eye of an impeller has been considered to be dependent on two factors, the effect of the shroud and the impeller vanes. To obtain the total maximum underpressure in the eye, the vane pressure drop is added to the pressure drop caused by the shroud. Reckoning in this manner, Spannhake and Wislicenus developed an expression for the cavitation index in the form

$$H_{sv} = \frac{K_1}{2g}\left(\frac{4Q}{\pi D^2}\right)^2 + \frac{K_2}{2g}\left[\left(\frac{4Q}{\pi D^2}\right)^2 + \left(\frac{ND}{60}\right)^2\right]$$

where K_1 and K_2 are shroud and vane coefficients, respectively, Q denotes the flow rate and D denotes the impeller diameter. Gongwer [2] was able to draw a mean line through his experimental data by properly selecting values for K_1 and K_2 and, in terms of the notation of this paper, his resulting empirical expression for cavitation index at head breakoff versus flow coefficient at zero incidence is

$$K_o = 1.4 + .085\left(1 + \frac{1}{\phi_o^2}\right)$$

Although this empirical equation represents Gongwer's experimental data for impellers having similar eye designs fairly well, it gives little insight into the mechanism involved and does not reflect the effect of such features as vane thickness or number and non-zero incidence angle of the flow.

An analytical method to calculate the complete flow field in an impeller is outlined in Ref. [7]. This stream filament technique was programmed on a large digital computer and used to design a number of mixed-flow impellers described in Ref. [6]. A comparison of the test results of these impellers with the theory showed the theory to have the proper general trends and give reasonably accurate results in the portion of the impeller where channel flow exists. However, in the inlet region of the impeller the theory gave pressures which were consistently too high, making it of little value for the prediction of cavitation.

Cavitation in impellers and inducers has generally been considered to be described by separated cavity flow at the leading edge of the vanes, similar to that which is observed in steady flow past a single foil. Analytical methods to describe this kind of cavitation breakdown [2], [3], [4] have been based on the model of a free-streamline flow through a cascade of flat plate hydrofoils. While this model is no doubt a reasonable representation of cavitating flow at large positive angles of incidence, it is of limited value near zero and at negative angles of incidence (overflows). The present theoretical findings indicate that at negative incidence a favorable pressure gradient exists and there is no tendency for a separated region to exist.

One of the first rather comprehensive contributions to the literature on pump cavitation was published by Gongwer [2]. A series of impellers of approximately the same eye design with widely differing outside diameters were tested with the

result that the effect of the differing outside diameter had no effect on cavitation. Thus, Gongwer concluded that the cavitation performance of an impeller is only dependent on the eye design and the angle of incidence that the fluid makes with the impeller vanes.

A simplified flow model advanced by Stanitz [5] to describe the effect of vane blockage at zero incidence was applied by Wood, Murphy and Farquhar [6] to their experimental results from mixed-flow pump tests. This model accounts for the reduced area caused by blockage effects of the vanes according to the one-dimensional continuity equation and relates the pressure at a station upstream of the impeller to the pressure at a station just inside the impeller according to the steady-flow form of Bernoulli's equation. The theoretical approach presented herein is essentially an extension of Stanitz's model to include the time derivative term in Bernoulli's equation.

The results of two outstanding experimental investigations of cavitation in mixed flow impellers are presented in the companion papers, Ref. [6] and [8]. The tests carried out under carefully controlled conditions showed the effect of vane incidence angle, thickness and number as well as speed effects. Since the geometrical characteristics of the series of impellers tested are well-recorded, the results were found to be very valuable for comparison with the theoretical result developed in this report.

THEORY

Two probable types of cavitation are hypothesized: (a) localized cavitation at the leading edge of the vanes, (b) gross cavitation behind the leading edge, which will be considered to be the true cavitation, giving rise to a significant reduction in performance. While the blunt leading edge part of the vanes is no doubt the critical point in the impeller, it is believed that cavitation here would be only a local phenomenon and probably would not result in a reduction in performance. Thus, we will consider the point just behind the leading edge as the critical point for gross cavitation and attempt a theoretical prediction of the pressure or cavitation index at this point.

In essence, the basic problem is to calculate the minimum pressure coefficient on the impeller under unsteady flow conditions. Assuming the flow to be incompressible and inviscid, Bernoulli's equation applied between some point in the inlet conduit, far enough removed from the impeller eye so that the flow can be considered locally steady, and some point within the impeller, gives:

$$1+\frac{P_o-P}{\frac{1}{2}\rho C_{mo}^2}=\left(\frac{q}{C_{mo}}\right)^2+\frac{2}{C_{mo}^2}\frac{\partial\phi}{\partial t}+\frac{2gh}{C_{mo}^2}$$

In this equation $\bar{q}$ is the local velocity measured with respect to a fixed reference frame. The subscript m denotes "meridonal" and "0" corresponds to the upstream reference point. The velocity potential ϕ is defined as $\bar{q}=\text{grad}\,\phi=\nabla\phi$. Neglecting the elevation term and adding and subtracting the fluid vapor

pressure, P_v, gives

$$\frac{P_o - P_v}{\frac{1}{2}\rho C_{mo}^2} + 1 - \frac{P - P_v}{\frac{1}{2}\rho C_{mo}^2} = \left(\frac{q}{C_{mo}}\right)^2 + \frac{2}{C_{mo}^2}\frac{\partial \Phi}{\partial t} \quad (1)$$

The classical theory of cavitation states that cavitation occurs when the local minimum pressure just equals the vapor pressure of the liquid. It is well-known, however, that in practice this simple concept is not always valid. Departures of the cavitation index from values calculated on the basis of this hypothesis are caused by so-called scale effects which arise from changes in size, velocity and fluid properties. Fortunately, however, experimental evidence indicates [9] that in the absence of *thermodynamic* effects the scale effects decrease with size and velocity so that for the prototype, this hypothesis yields valid results. Thus, proceeding on the basis that the size and speed of the impeller are sufficiently large so that the condition of cavitation is reached when $P = P_v$, equation (1) may be written

$$K_o = \left(\frac{q}{C_{mo}}\right)^2 + \frac{2}{C_{mo}^2}\frac{\partial \Phi}{\partial t} \quad (2a)$$

where

$$K_o = \frac{P_o - P_v}{\frac{1}{2}\rho C_{mo}^2} + 1 \quad (2b)$$

is defined as the cavitation index. The cavitation index in this formulation is exactly equal to one minus the minimum pressure coefficient. Unfortunately, this definition differs by a factor of 1.0 with the index, σ, which is in common use for uniform flow past bodies such as head forms and hydrofoils.

It is, however, consistent with the definition generally used for turbomachinery.

According to equation (2) it is evident that in order to calculate the cavitation index, it is necessary to evaluate both the absolute local velocity, $\bar{q}$, and $\frac{\partial \Phi}{\partial t}$ at the critical location on the impeller. As a first approximation, $\bar{q}$ may be taken to be the meridional velocity at the point in question, which will be dependent on the shroud and hub configuration, corrected for vane blockage. The effect of vane thickness can be approximated by accounting for the reduction in flow area presented by the vanes according to one-dimensional flow principles.

The term $\partial\Phi/\partial t$ can also be approximated once $\bar{q}$ is known provided the kind of unsteady flow involved is recognized. That is, although the flow is unsteady when viewed from a fixed reference frame, it is steady in a reference frame rotating with the impeller. As a consequence, we may imagine a velocity potential field fixed to and rotating with the impeller. The term $\partial\Phi/\partial t$, which denotes the time derivative of Φ measured in the fixed reference frame, may be calculated by observing the change in Φ as the Φ-field rotates past a point fixed in space during a small time interval.

If the vane thickness was zero and the vanes were aligned with the flow, the surfaces of constant Φ would represent disks or surfaces axisymmetric with respect to the impeller axis. In this case $\frac{\partial \Phi}{\partial t}$ would vanish since an observer fixed in space would observe only one value of Φ as these disks are rotated. However, when the vanes have a finite thickness or are operated

at some angle of incidence, the flow is disturbed and the surfaces of constant Φ are distorted so that they are no longer axisymmetric. In this case $\frac{\partial \Phi}{\partial t}$ would no longer be zero.

Figure 1 shows a schematic of the unperturbed flow where the vane thickness is zero and the vanes are perfectly aligned with the flow. In this case $C_{m1}=C_{m2}$ and the velocity potential lines are aligned with the vane velocity vector as indicated. For the flow depicted here, $\partial\Phi/\partial t=0$ because the lines corresponding to constant values of Φ move in the direction of their orientation. An observer fixed in space would observe the same value of Φ as time progresses and the velocity potential field rotates. For this special unperturbed condition the cavitation index as given by equation (2) reduces to

$$K_o=(C_{m1}/C_{mo})^2$$

This relationship which represents the lower limit of K_o reflects only the effect of the shroud on cavitation index since the vanes have no thickness and are aligned with the flow.

Figure 2 illustrates the case of finite vane thickness, i.e., a small perturbation of the flow depicted in Figure 1. For this case it is evident that $C_{m2}>C_{m1}$ where C_{m2} may be related to C_{m1} approximately by the one-dimensional continuity relationship

$$C_{m2}=\frac{C_{m1}}{1-B_v} \qquad (3)$$

where the vane blockage coefficient, B_v, represents the ratio of the vane frontal area to the area of the passage without

vanes. For purposes of evaluating B_v the projected vane frontal width is taken as $\tau/\sin\beta$ where τ is the vane thickness and β is the local vane angle indicated in Figure 2. Since C_{m2} is greater than C_{m1} and $C_m = \frac{\partial \Phi}{\partial x}$, the velocity potential lines must be more closely spaced in the axial direction for finite vane thickness. Nevertheless, the basic kinematic boundary condition on the surface of the vane, given by

$$\frac{\partial \Phi}{\partial n} = \bar{u} \cdot \bar{n} = -u \sin\beta \qquad (4)$$

where $\bar{n}$ denotes the unit normal vector to the blade and $\bar{u}$ denotes the local vane velocity vector, must still be satisfied as it was for the case of zero vane thickness. That is, in either case the normal derivative of the velocity potential must satisfy the condition:

$$\left.\frac{\partial \Phi}{\partial n}\right|_{\tau=0} = \left.\frac{\partial \Phi}{\partial n}\right|_{\tau=\text{finite}} = -u \sin\beta$$

From this condition, then, the new Φ_1 and Φ_2 lines for the perturbated, flow having the same values as those indicated in Figure 1, can be drawn. Thus, in Figure 2 we have represented by dashed lines the new Φ_1 and Φ_2 lines which are more closely spaced in the x-direction as required since $C_{m2} > C_{m1}$ but still having the same value of $\frac{\partial \Phi}{\partial n}$ on the vane surface. That is, to satisfy this normal derivative requirement the new Φ lines are constructed so as to intersect points B and C in Figure 2.

To evaluate $\frac{\partial \Phi}{\partial t}$, $\Delta\Phi$ can be written as $\Delta\Phi = \Phi_2 - \Phi_1 = \frac{\partial \Phi}{\partial x} \Delta x'$ where $\Delta x'$ is the axial distance indicated in Figure 2. The corresponding Δt is $\Delta t = \frac{\Delta c}{u}$ where Δc is the distance indicated in

Figure 2 and u is the vane velocity. Thus,

$$\frac{\partial \Phi}{\partial t} = \frac{\Delta \Phi}{\Delta t} = \frac{\frac{\partial \Phi}{\partial x} \Delta x'}{\frac{\Delta c}{u}} = u \frac{\partial \Phi}{\partial x} \frac{\Delta x'}{\Delta c} \tag{5}$$

but, as indicated in Figure 2,

$$\frac{\Delta x'}{\Delta c} = \tan \theta \simeq \theta \tag{6}$$

for small values of θ. Thus, from equation (5) and (6) $\frac{\partial \Phi}{\partial t}$ can be written,

$$\frac{\partial \Phi}{\partial t} = U C_{m2} \theta \tag{7}$$

where $\frac{\partial \Phi}{\partial x}$ has been replaced by C_{m2}.

By definition of the velocity potential, $\frac{\partial \Phi}{\partial n}$ is equal to the velocity of the fluid in a direction normal to the vane surface. From Figure 2 it is evident that this can be written as

$$\frac{\partial \Phi}{\partial n} = \frac{\frac{\partial \Phi}{\partial x}(-\Delta x')}{\Delta n} = - \frac{\partial \Phi}{\partial x} \frac{\Delta x'}{\Delta x} \cos\beta \tag{8}$$

Considering the geometry of the triangle (BCD), indicated in Figure 2, it is evident that

$$a = \Delta x \tan\beta \tag{9}$$

and

$$\Delta x - \Delta x' = a \tan\theta \simeq a\theta \tag{10}$$

Eliminating a between equations (9) and (10) and substituting this result into equation (8) gives

$$\frac{\partial \Phi}{\partial n} = - \frac{\partial \Phi}{\partial x} (1 - \theta \tan\beta) \cos\beta \tag{11}$$

Substituting this expression for $\frac{\partial \Phi}{\partial n}$ into the kinematic boundary condition given in equation (4) yields

$$\Theta = \cot\beta - \frac{u}{C_{m2}}$$

where, again, $\frac{\partial \Phi}{\partial x}$ has been replaced by C_{m2}. Substituting this expression into equation (7) yields the following expression for $\frac{\partial \Phi}{\partial t}$ in terms of the vane velocity, angle and meridional velocity:

$$\frac{\partial \Phi}{\partial t} = u\, C_{m2}\left(\cot\beta - \frac{u}{C_{m2}}\right) \tag{12}$$

Finally, substituting the relationship given in equation (12) for $\frac{\partial \Phi}{\partial t}$ and using the approximation $q=C_{m2}$ in equation (2) yields the following relationship for the cavitation index:

$$K_o = \left(\frac{C_{m2}}{C_{mo}}\right)^2 + 2\,\frac{u}{C_{mo}}\,\frac{C_{m2}}{C_{m1}}\left(\cot\beta - \frac{u}{C_{m2}}\right) \tag{13}$$

Since, in general, the upstream reference velocity, C_{mo}, and the local shroud velocity for zero vane thickness, C_{m1}, differ due to the effect of the shroud, it is convenient to introduce C_{m1} into equation (13) to obtain

$$K_o = \left(\frac{C_{m1}}{C_{mo}}\right)^2\left(\frac{C_{m2}}{C_{m1}}\right)^2 + 2\,\frac{1}{\phi_o}\,\frac{C_{m2}}{C_{m1}}\left(\cot\beta - \frac{1}{\phi_o}\,\frac{C_{mo}}{C_{m1}}\,\frac{C_{m1}}{C_{m2}}\right) \tag{14}$$

where $\phi_o = C_{mo}/u$ is the flow coefficient based on the upstream meridional velocity. C_{m1}/C_{mo} can be called a shroud coefficient since, from a one-dimensional flow point of view, it represents the ratio of the inlet pipe reference area to the local passage area if vanes are not present. C_{m2}/C_{m1} can be called a vane coefficient since it represents the ratio of the local passage area without and with vanes, respectively. From one-dimensional continuity considerations, as given in

equation (3),

$$C_v = \frac{C_{m2}}{C_{m1}} = \frac{1}{1-B_v} = \text{vane coefficient} \qquad (15)$$

and

$$C_s = \frac{C_{m1}}{C_{mo}} = \frac{A_o}{A_1} = \text{shroud efficient} \qquad (16)$$

where B_v is the vane blockage coefficient and A_o/A_1 is the area of the reference section in the inlet pipe to the local area of the passage excluding the effect of vane blockage. Using these definitions, the final expression for the cavitation index becomes

$$K_o = C_s^2 C_v^2 + 2 C_v \cot\beta \frac{1}{\phi_o} - \frac{2}{C_s} \frac{1}{\phi_o^2} \qquad (17)$$

Equation (17) relates the cavitation index to vane and shroud coefficients, the vane angle and the flow coefficient. The first term represents the dynamic depression associated with the velocity-squared term in the Bernoulli's equation while the second two terms together represent the contribution from the unsteady term. The equation is valid at any radial location on the vane if β and ϕ_o are interpreted as the local vane angle and local flow coefficient, respectively. However, numerical evaluation of the equation shows that the maximum value of K_o occurs at the vane tip as might be expected. Accordingly, β and ϕ_o should be interpreted as the vane setting angle and ratio of C_{mo} to the vane wheel speed at the vane tip, respectively. It may be noted also that, although the "suction" side of the vane was used in the analysis, the resulting equation is the same regardless of which side is employed. It is only necessary that

β be interpreted as the angle of the vane face in question if they are different.

As indicated previously the cavitation index is, by definition, related to the minimum value of the pressure coefficient according to

$$K_o = 1 - C_{p(min)}$$

where $C_{p(min)}$ is based on the pressure and velocity at the upstream sub "o" reference station. A value of $K_o = 1.0$ therefore corresponds to the condition where the local pressure is equal to the upstream reference pressure. This, of course, would correspond to the minimum possible value of the cavitation index excluding effects of both the vanes and shroud. Values of K_o less than unity would simply indicate that the local pressure was greater than the reference pressure and, these values are of no significants.

The condition where the flow just inside the vanes at station "2" is aligned with the vanes is of particular interest. This condition is defined by $\phi_2 = \tan\beta$ or, equivalently, $\phi_o = \tan\beta / C_s C_v$. Substituting this value for ϕ_o into equation (17) yields simply

$$K_o = C_s^2 C_v^2 \qquad (18)$$

because the second and third terms, corresponding to the contribution of $\partial\Phi/\partial t$, cancel each other. This result is essentially that of the blockage model proposed by Stanitz [5].

Values of ϕ_o which are less than $\tan\beta / C_s C_v$ correspond to underflows or positive incidence at the vanes and the contribution from $\partial\Phi/\partial t$ in equation (17) is negative, tending to decrease

K_o. This effect, interpreted in terms of local pressure, corresponds to an increase in pressure and pressure coefficient. Although the measurements [6] show that the average pressure inside the vanes does, in fact, increase for the positive incidence condition, it is also clear that the measured cavitation index increases, indicating a local depression. It is understandable then that Equation (17), which is based on one-dimensional flow considerations, disregards the local anomolies due to leading edge flow and predicts the increase in pressure at stations behind the leading edge. This positive incidence flow is discussed in more detail and in relation to experimental findings in a later section.

Flow at values of ϕ_o which are greater than $\tan\beta/C_s C_v$ corresponds to underflow or a negative incidence at the leading edge of the vanes. For this condition the last two terms in equation (17), which represent the contribution from $\partial\Phi/\partial t$, give a positive contribution to K_o. This effect, when interpreted in terms of pressure, corresponds to a depression and, consequently, reduced cavitation performance.

COMPARISON WITH EXPERIMENTAL RESULTS

Figures 3,4,5 and 6 show the experimental results from mixed-flow pump tests of Wood, Murphy and Farquhar [6] and Wood [8] along with the present theoretical results obtained from equation (17). The experimental points represent values of the cavitation index as a function of the flow coefficient at the condition where the head rise curve just began to

decrease due to cavitation. The details of the impeller geometries are given in Ref. [6] and [8] and, for purposes of application of equation (17), the features indicated in Table 1 were taken from these references.

TABLE 1-IMPELLER INLET GEOMETRY

Impeller	No. of Vanes	Tanβ at Vane Tip (suction side)	(pressure side)	(Ave.)	B_v	C_v	C_s
C	4	.291	.321	.306	.0703	1.075	1.04
B	5	.299	.329	.314	.088	1.095	1.04
A	6	.326	.336	.331	.105	1.118	1.04
D	8			.46	.1403	1.163	1.04

It may be noted that tanβ in Table 1 has two different values at the tip. This is due to the fact that the vanes were not of constant thickness but increased in width with distance from the leading edge.

One particularly noteworthy feature of the experimental data is the so-called velocity scale effect. The experimental cavitation index in Figure 3-6 shows a decrease with impeller rotative speed with the higher speed runs showing the better agreement with the present theory. The authors of Ref. [6] indicate that this velocity scale effect has an upper limit, however, since no distinct speed effect was observed in a comparison of the 4920 rpm runs with some higher speed runs at 6500 rpm. It may be noted that this kind of dependence on speed has also been found in other experimental data for submerged bodies and, in general, the velocity scale effect has been found to decrease with velocity so that

eventually K_o approaches $1-C_{p(min)}$. In other words, the cavitation index approaches the value as calculated on the hypothesis that cavitation occurs when the local pressure equals the vapor pressure. Since this classical hypothesis was the basis for the present theory the agreement with the high speed runs is encouraging.

The three vertical line on Figure 3,4,5 and 6 are of special interest when comparing the present theory with the experimental results. The one line labled $\phi_o=\tan\beta$ denotes the value of ϕ_o where the flow at the upstream reference station is such that the relative flow angle with the vanes would be zero. However, when the fluid encounters the vane leading edges it no longer has the velocity of C_{mo} but has velocity C_{m1} due to the effect of the shroud. Thus, the condition of $\phi_1=\tan\beta$ (or $\phi_o=\tan\beta/C_s$)has more significance than $\phi_o=\tan\beta$ since the former indicates the condition where the flow is approaching the vane leading edges at zero incidence. However, as pointed out by the authors of Ref. [6], this condition still is not the true condition of zero incidence, since due to vane blockage, the relative flow just inside the vane row would not be tangent to the vanes. The true zero-incidence condition occurs when $\phi_2=\tan\beta$ or $\phi_o=\tan\beta/C_sC_v$. For this condition equation (17) reduces to

$$K_o=C_s^2C_v^2$$

which correpsonds to the minimum value of K_o. This value of ϕ_o is also indicated in the figures as a vertical line.

The authors of Ref. [6] have pointed out that their experimental data shows that the best cavitation performance, which corresponds to the minimum value of K_o, occurs at the zero incidence condition of $\phi_2 = \tan\beta$. Equation (17) corroborates this conclusion to the extent that K_o decreases with decreasing values of ϕ_o. When $\phi_2 = \tan\beta$ or $\phi_o = \tan\beta/C_s^2 C_v$ the cavitation index becomes $K_o = C_s^2 C_v$ because the second and third terms, which arise on account of the $\partial\phi/\partial t$ term in Bernoulli's equation, cancel each other. However, for values of ϕ_o smaller than $\tan\beta/C_s^2 C_v$, equation (17) shows a continued decrease in K_o while the experimental data show a minimum at $\phi_o = \tan\beta/C_s^2 C_v$ with a subsequent rise with decreasing values of ϕ_o. This continued decrease of K_o with decreasing values of ϕ_o simply indicates that the $\partial\phi/\partial t$ term occurring in Bernoulli's equation gives rise to an increase in pressure over that existing at station 1. Although it is evident that K_o could never drop below C_s^2 (corresponding to cavitation outside the vanes at station 1) experiments show a rapid increase in K_o below $\phi_o = \tan\beta/C_s^2 C_v$. This rather extreme departure seems to indicate that some other mechanism is responsible for the cavitation breakdown at positive incidence angles.

The difference between the theory and experimental data occurring at positive angles of incidence, that is, at values of $\phi_o = \tan\beta/C_s^2 C_v$ is not without an explanation. The one possible explanation which presents itself is that for positive incidence the pressure, as calculated according to the present theory, increases just inside the vane row. (This is born out by pressure measurements of Ref. [6].) This pressure increase in the direction

of the flow (or adverse pressure gradient) would naturally tend to result in leading edge stall. However, for negative incidence the present theory shows a decrease in pressure as indicated by the rising value of K_o with ϕ_o. This reduction in pressure inside the vane row would provide a favorable pressure gradient and, consequently, the result would be a well-behaved, attached flow. Thus, although at the outset there may seem to be no difference between positive and negative angles of incidence, as would be the case in steady cascade flow, the $\partial\Phi/\partial t$ term in Bernoulli's equation gives rise to an adverse pressure gradient in the one instance and a favorable pressure gradient in the other. As a consequence, the resulting flow is apparently altogether different for the two possible incidence conditions.

SUMMARY AND CONCLUSIONS

A potential flow theory has been developed to predict cavitation in pump impellers which takes into account the unsteady term occurring in Bernoulli's equation. The theory has been applied to mixed-flow pump impellers and test results show good agreement near the zero incidence and overflow condition. As the relative flow angle of attack increases the theoretical and experimental results diverge due apparently to the predominance of the leading edge cavity in causing performance reduction.

Figure 7 is an attempt to depict the salient features of cavitation breakdown in pump impellers. At $\phi_o = \tan\beta / C_s C_v$ as indicated on the figure the unsteady term in Bernoulli's equation causes no pressure reduction, and equation (17) yields simply $K_o = C_s^2 C_v^2$. This point is referred to as the point of zero incidence. For points to the right of this point, corresponding to values of negative incidence, the one-dimensional theory, which disregards local effects at the vane leading edge, shows reasonable agreement with the experimental results. This agreement is apparently attributable to the flow stabilizing effect of the favorable pressure gradient caused by the $\partial\Phi/\partial t$ term occurring in Bernoull's equation. Points to the left of the point $\phi_o = \tan\beta / C_s C_v$ correspond to values of positive incidence. The sharply decreasing K_o versus ϕ_o curve with increasing incidence angle, α, indicates the existence of the adverse pressure gradients in the inlet region. This adverse pressure gradient apparently results in leading edge stall, a phenomenon

which would tend to block the flow passage and result in drastic performance deterioration.

Although the present theory does not predict the minimum value of the cavitation index with acceptable accuracy it does shed some light on a very difficult and important problem. At overflow (or negative incidence) conditions the unsteady term in Bernoulli's equation has been shown to provide a very important contribution to the pressure reduction in the inlet region and the theoretical results generally agree with the experimental data. At underflow the time derivative term contributes to an adverse pressure gradient.

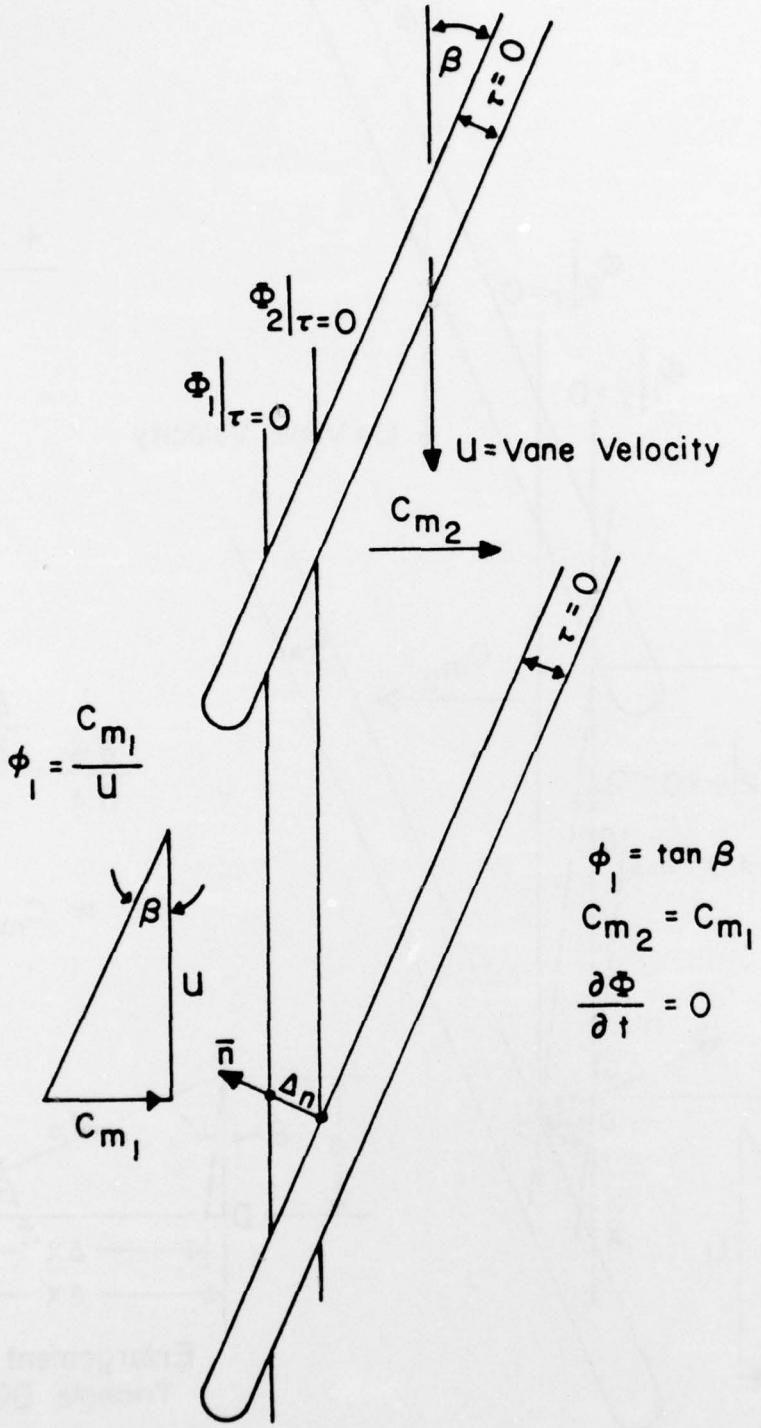

FIGURE 1. VELOCITY POTENTIAL FIELD ROTATING WITH IMPELLER - ZERO VANE THICKNESS AND INCIDENCE ANGLE.

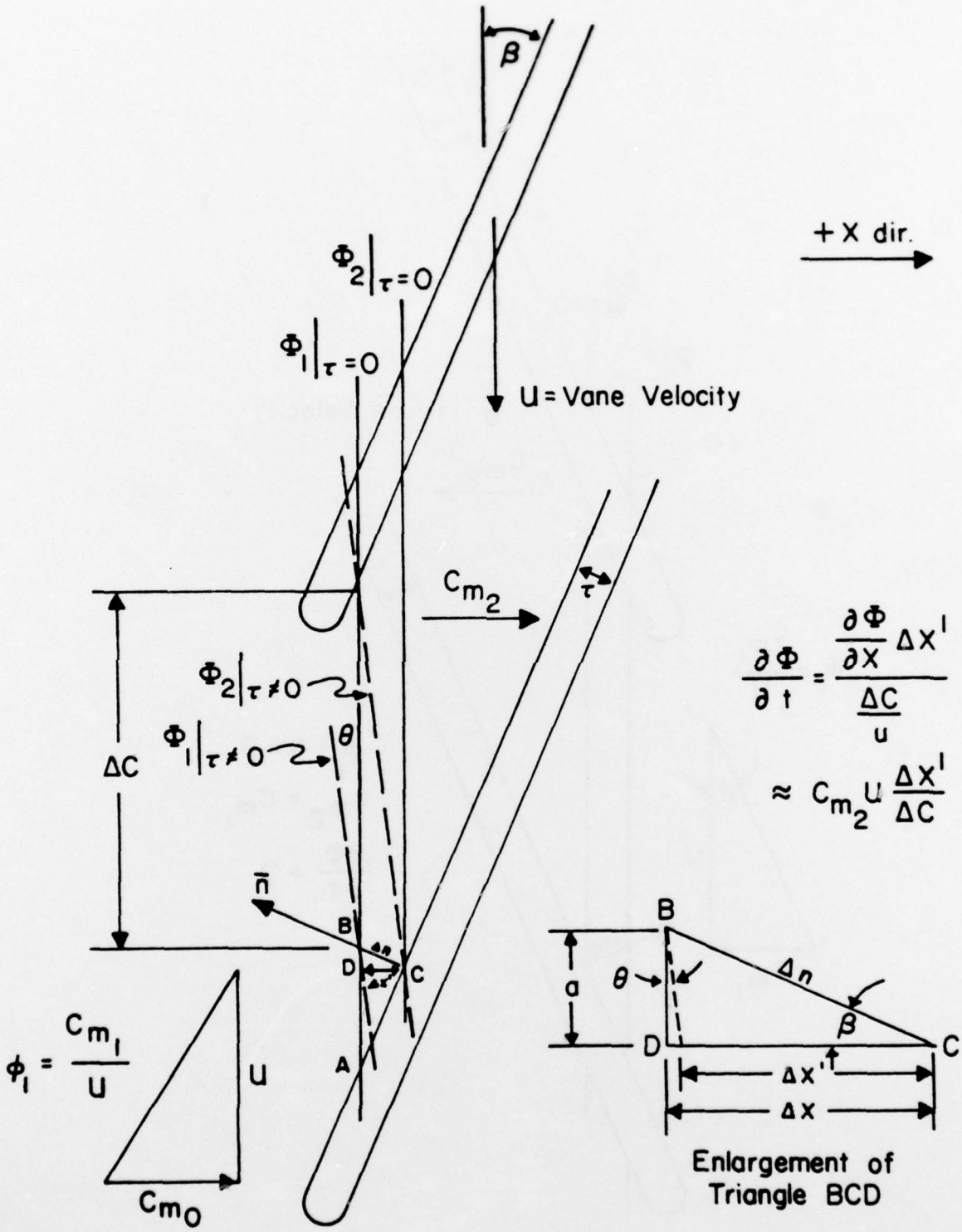

FIGURE 2. VELOCITY POTENTIAL FIELD ROTATING WITH IMPELLER.

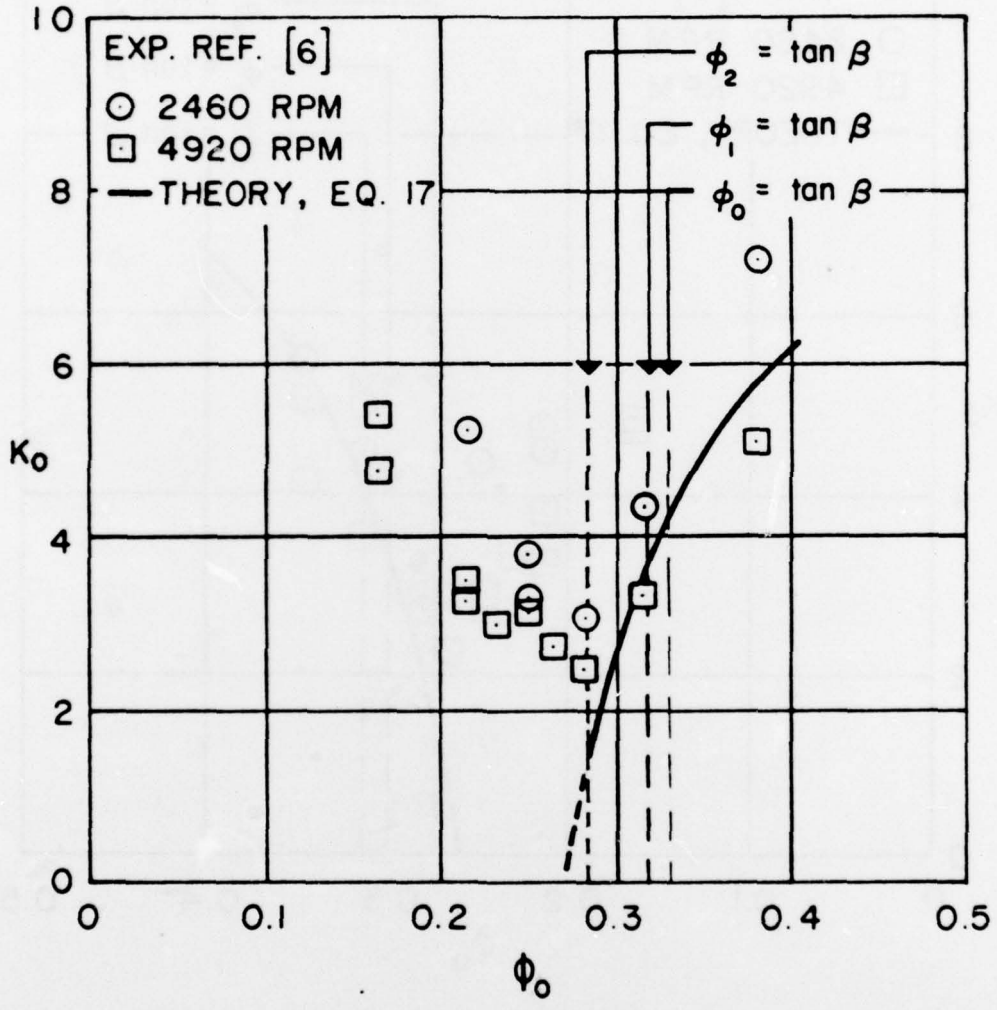

FIGURE 3. CAVITATION INDEX VERSUS FLOW COEFFICIENT — IMPELLER A.

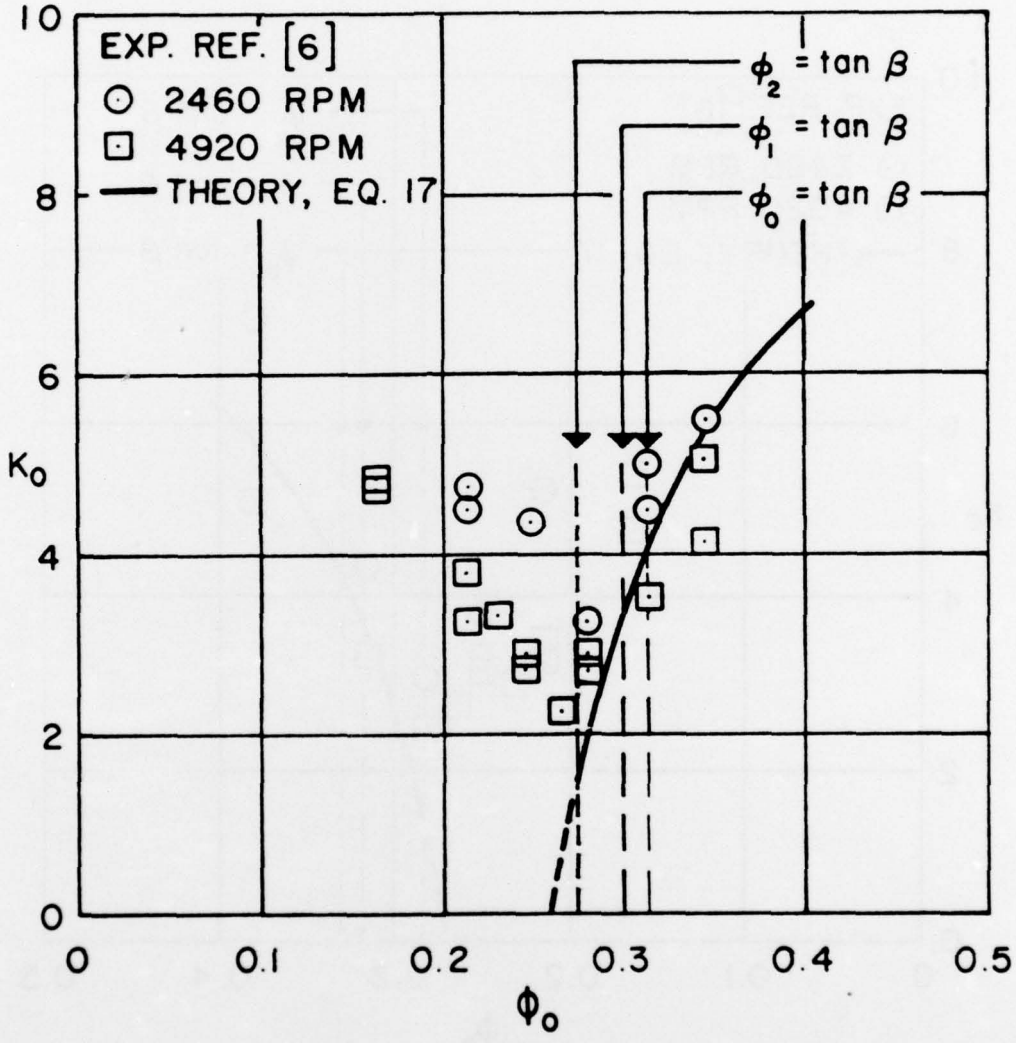

FIGURE 4. CAVITATION INDEX VERSUS FLOW COEFFICIENT – IMPELLER B.

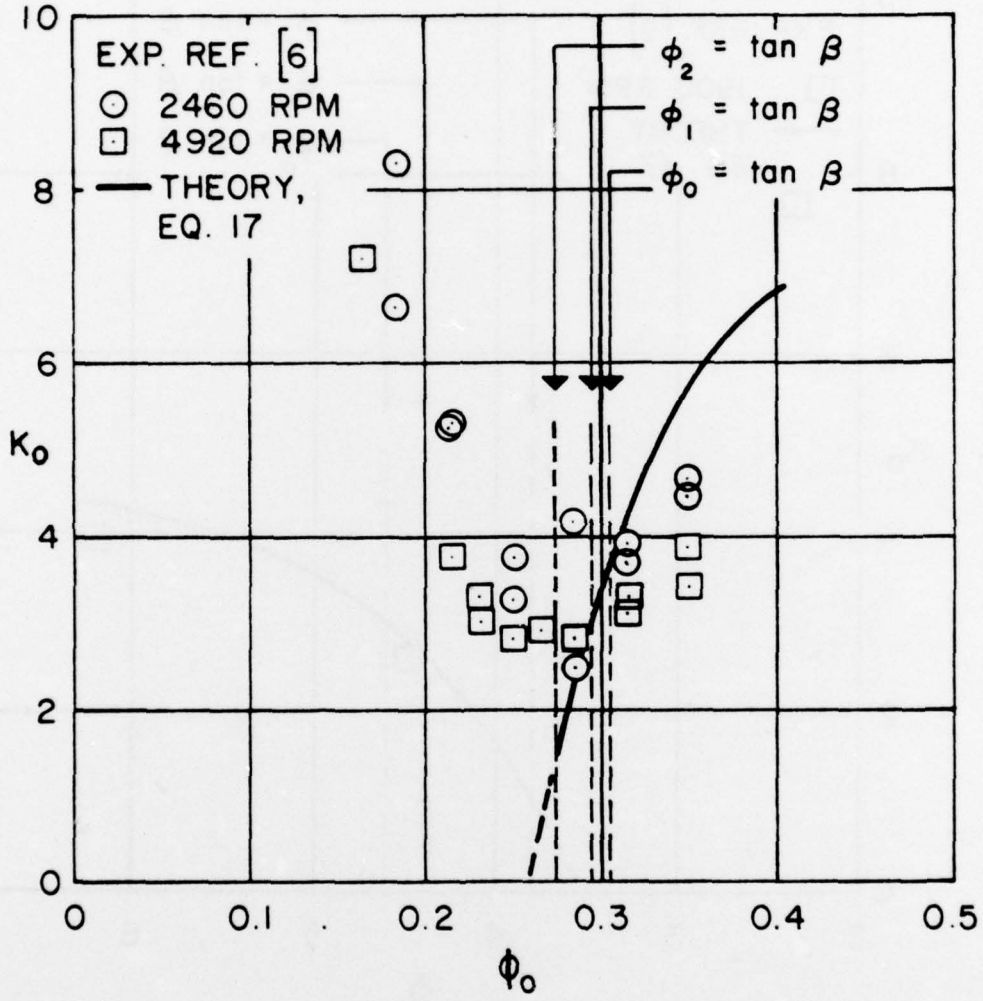

FIGURE 5. CAVITATION INDEX VERSUS FLOW COEFFICIENT — IMPELLER C.

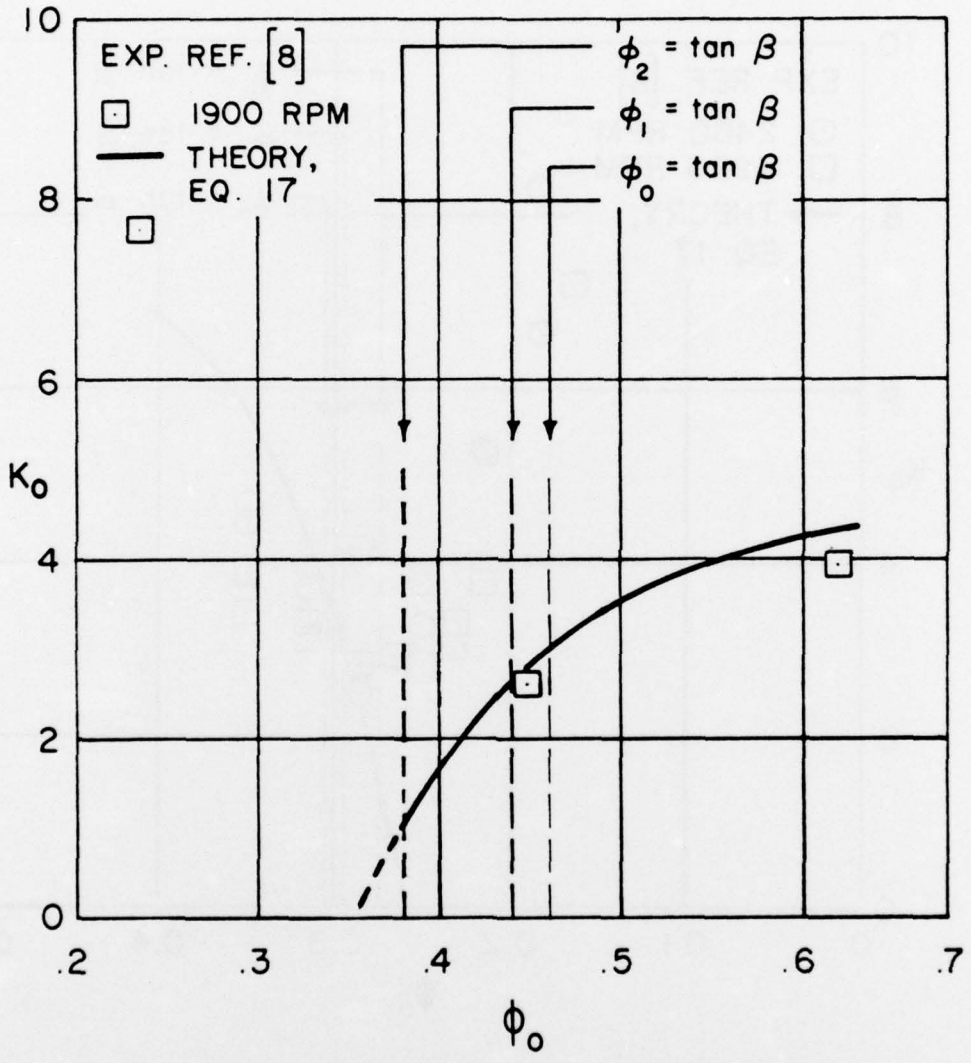

FIGURE 6. CAVITATION INDEX VERSUS FLOW COEFFICIENT - IMPELLER D.

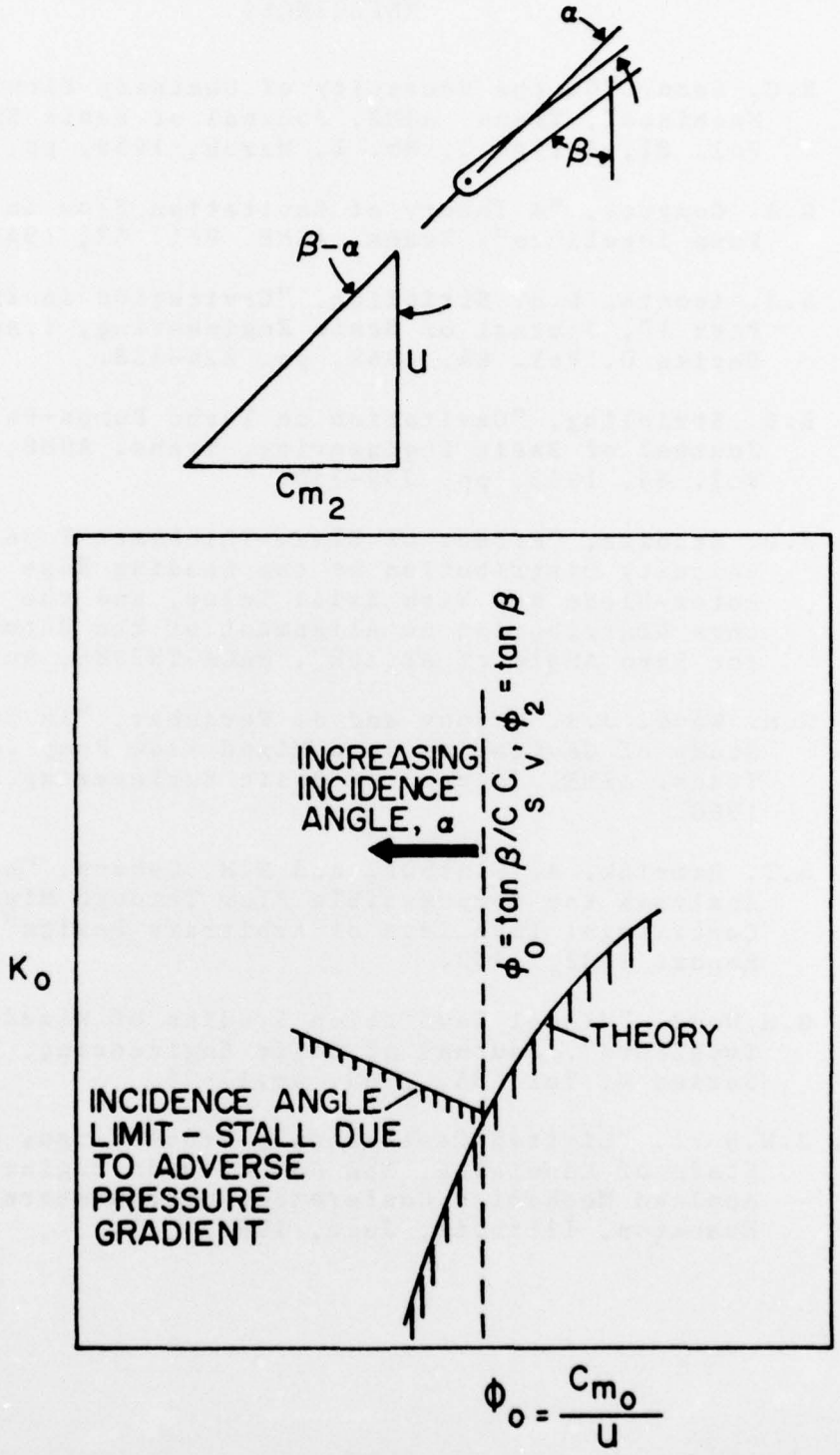

FIGURE 7. CAVITATION INDEX VERSUS FLOW COEFFICIENT.

REFERENCES

1. R.C. Dean, "On the Necessity of Unsteady Flow in Fluid Machines", Trans. ASME, Journal of Basic Engineering, Vol. 81, Series D, No. 1, March, 1959, pp. 24-48.

2. C.A. Gongwer, "A Theory of Cavitation Flow in Centrifugal-Pump Impellers", Trans. ASME, Vol. 63, 1941, pp. 29-40.

3. A.J. Acosta, L.B. Stripling, "Cavitation in Turbo Pumps-Part I", Journal of Basic Engineering, Trans. ASME, Series D, Vol. 84, 1962, pp. 326-338.

4. L.B. Stripling, "Cavitation in Turbo Pumps-Part II", Journal of Basic Engineering, Trans. ASME, Series D, Vol. 84, 1962, pp. 339-350.

5. J.D. Stanitz, "Effect of Blade-Thickness Taper on Axial-Velocity Distribution at the Leading Edge of an Entrance Rotor-Blade Row With Axial Inlet, and the Influence of this Distribution on Alignment of the Rotor Blade Angle for Zero Angle of Attack", NACA TN2986, August, 1953.

6. G.M. Wood, J.S. Murphy and J. Farquhar, "An Experimental Study of Cavitation in a Mixed Flow Pump Impeller", Trans. ASME, Journal of Basic Engineering, December, 1960.

7. J.T. Hamrick, A. Ginsburg and W.M. Osborn, "Method of Analysis for Compressible Flow Through Mixed-Flow Centrifugal Impellers of Arbitrary Design", NACA Report 1082, 1953.

8. G.M.Wood, "Visual Cavitation Studies of Mixed-Flow Pump Impellers", Journal of Basic Engineering, Trans. ASME, Series D, Vol. 85, 1963, pp.17-28.

9. J.W.Holl, "Limited Cavitation", Proceedings, Cavitation State of Knowledge, The ASME Fluids Engineering and Applied Mechanics Conference, Northwestern University, Evanston, Illinois, June, 1969.

DISTRIBUTION LIST

Defense Documentation Center (DDC) Cameron Station Alexandria, VA 22314	2
Library Naval Postgraduate School Monterey, CA 93940	2
Dean of Research (Code 012) Naval Postgraduate School Monterey, CA 93940	1
Mr. Ross Hatte Naval Systems Division The Boeing Company Seattle, Washington	1
Prof. J.W.Holl *Ordnance Research Laboratory* Penn. State University P.O. Box 30 State College, Pennsylvania 16801	1
Prof. R.E. Nece Department of Civil Engineering University of Washington Seattle, Washington	1
Glenn M. Wood Pratt & Whitney Aircraft Division of United Aircraft Corporation East Hartford, Connecticut 06108	1
F.F. Antunes Cameron Engineering Department Ingersoll Rand Company Pillipsburg, New Jersey 08865	1
C.J.Garrison *Department of Mechanical Engineering* Naval Postgraduate School Monterey, California 93940	10

Department of Mechanical Engineering
Naval Postgraduate School
Monterey, California 93940

1